OXFORD UNIVERSITY PRESS | Human Molecular Genetics

Loss of HCN1 enhances disease progression in CNG channel-linked retinitis pigmentosa and achromatopsia

Journal:	*Human Molecular Genetics*
Manuscript ID	Draft
Manuscript Type:	2 General Article - UK Office
Date Submitted by the Author:	n/a
Complete List of Authors:	Schön, Christian; Ludwig-Maximilians-Universität München, Department of Pharmacy – Center for Drug Research Asteriti, Sabrina; University of Pisa, Department of Translational Research Koch, Susanne; Ludwig-Maximilians-Universität München, Department of Pharmacy – Center for Drug Research Sothilingam, Vithiyanjali; Institute for Ophthalmic Research, Ocular Neurodegeneration Garcia Garrido, Marina; Institute for Ophthalmic Research, Ocular Neurodegeneration Tanimoto, Naoyuki; University of Tuebingen, Division of Ocular Neurodegeneration, Inst. for Ophthalmic Research; Herms, Jochen; Ludwig Maximilians University , Neuropathology Seeliger, M.; Inst. for Ophthalmic Research, Division of Ocular Neurodegeneration Cangiano, Lorenzo; University of Pisa, Department of Translational Research Biel, Martin; Ludwig-Maximilians-Universität München, Department of Pharmacy Michalakis, Stylianos; Ludwig-Maximilians-Universität München, Department of Pharmacy – Center for Drug Research
Key Words:	retinitis pigmentosa, achromatopsia, photoreceptor degeneration, optical coherence tomography, hyperpolarization-activated cyclic nucleotide-gated channel

SCHOLARONE™
Manuscripts

Loss of HCN1 enhances disease progression in CNG channel-linked retinitis pigmentosa and achromatopsia

Christian Schön[1], Sabrina Asteriti[2], Susanne Koch[1], Vithiyanjali Sothilingam[3], Marina Garcia Garrido[3], Naoyuki Tanimoto[3], Jochen Herms[4,5], Mathias W. Seeliger[3],Lorenzo Cangiano[2], Martin Biel[1], Stylianos Michalakis[1]

[1]Center for Integrated Protein Science Munich CiPS[M] at the Department of Pharmacy – Center for Drug Research, Ludwig-Maximilians-Universität München, Munich, Germany

[2]Department of Translational Research, University of Pisa, Pisa, Italy

[3]Division of Ocular Neurodegeneration, Institute for Ophthalmic Research, Centre for Ophthalmology, University of Tübingen, Schleichstr. 4/3, 72076 Tübingen, Germany.

[4]German Center for Neurodegenerative Diseases-Munich site (DZNE-M) and Center for Neuropathology and Prion Research (ZNP), Ludwig-Maximilians-Universität München, Munich

[5]Munich Cluster of Systems Neurology (SyNergy), Ludwig-Maximilians-Universität München, Munich, Germany

Correspondence to: michalakis@lmu.de

For Peer Review

Abstract

Most inherited blinding diseases are characterized by compromised retinal function and progressive degeneration of photoreceptors. However, the factors that affect the life span of photoreceptors in such degenerative retinal diseases are rather poorly understood. Here we explore the role of hyperpolarization-activated cyclic nucleotide-gated channel 1 (HCN1) in this context. HCN1 is known to adjust retinal function under mesopic conditions, and although it is expressed at high levels in rod and cone photoreceptor inner segments, no association with any retinal disorder has yet been found. We investigated the effects of an additional genetic deletion of HCN1 on the function and survival of photoreceptors in a mouse model of *CNGB1*-linked retinitis pigmentosa (RP). We found that the absence of HCN1 in *Cngb1* knockout (KO) mice exacerbated photoreceptor degeneration. The deleterious effect was reduced by expression of HCN1 using a viral vector. Moreover, pharmacological inhibition of HCN1 also enhanced rod degeneration in *Cngb1* KO mice. Patch-clamp recordings revealed that the membrane potentials of *Cngb1* KO and *Cngb1*/*Hcn1* double KO rods were both significantly depolarized. We also found evidence for altered calcium homeostasis and increased activation of the protease calpain in *Cngb1*/*Hcn1* double KO mice. Finally, the deletion of HCN1 also exacerbated degeneration of cone photoreceptors in a mouse model of *CNGA3*-linked achromatopsia. Our results identify HCN1 as a major modifier of photoreceptor degeneration and suggest that pharmacological inhibition of HCN channels may enhance disease progression in RP and achromatopsia patients.

For Peer Review

Introduction

Retinal neurodegeneration is a key feature of many inherited blinding eye diseases with high clinical and socioeconomic impact. The degenerative process often concerns the photoreceptors and can be of cell autonomous or non-cell autonomous nature. A large number of disease causing mutations have been identified (https://sph.uth.edu/retnet) and some mechanistic insights on disease-related functional defects (e.g. lack of photoresponse in the absence of cyclic nucleotide-gated (CNG) channels (1)) have been gained (2-4).

Photoreceptors are retinal neurons specialized on the detection of light and the translation of light encoded information into electrical activity in a process called phototransduction. The photoreceptor membrane potential is controlled by CNG channels found in the plasma membrane of photoreceptor outer segments (5). Moreover, a number of proteins mediate or modulate additional ion conductances and help adjusting the electrical properties of photoreceptors (6-8). One of those proteins is the hyperpolarization-activated cyclic nucleotide-gated (HCN) channel found in photoreceptor inner segments. Four HCN channel genes (*Hcn1-4*) exist (9) and all of them are expressed in the mammalian retina with distinct patterns of localization (10). Among the *Hcn* channel genes, *Hcn1* shows the highest expression levels in photoreceptors and, overall, is one of the most highly expressed retinal genes (11). The HCN1 channel is strongly enriched in rod and cone photoreceptor inner segments where it contributes to shaping the photoresponse (12-14). In line with this, genetic deletion of *Hcn1* in mice results in prolongation of the scotopic and photopic electroretinogram (ERG) responses (14). Moreover, in the absence of HCN1 sustained rod responses after bright light illumination saturate the retinal network and impair downstream cone signaling (15). Systemic pharmacological inhibition of HCN channels in animal models also results in characteristic changes in the ERG responses (16, 17). Ivabradine, the first clinically approved hyperpolarization activated current (I_h) inhibitor acting on HCN channels is used for the treatment of stable angina pectoris (18). In agreement with the functional role

For Peer Review

of HCN1 in shaping the retinal photoresponse, about 15 % of the patients report the occurrence of light-stimulus-independent visual sensations, so called phosphenes, under ivabradine medication (19, 20). Therefore, it is suggested to exercise caution when prescribing ivabradine to patients with chronic retinal diseases like retinitis pigmentosa (RP). RP is a hereditary ocular disorder characterized by progressive degeneration of rod photoreceptors. Secondary to rods, cone photoreceptors also degenerate by an unknown non-cell-autonomous mechanism (21). The disease progression can vary significantly between patients, and the severity mainly depends on the nature of the disease causing gene mutation but can also be influenced by additional confounding factors.

We hypothesized that proteins controlling the electrical properties of photoreceptors might also influence the disease progression. Given the high levels of expression and its important physiological role in retinal photoreceptors HCN1 was our major candidate. To analyze the importance of HCN1 for photoreceptor cell viability in the context of degenerative retinal diseases we cross-bred retinal degeneration mouse models with mice lacking the *Hcn1* gene and followed the disease progression using *in vivo* and *in vitro* techniques. In addition, we explored the effect of pharmacological inhibition of HCN channels in retinal degeneration.

We show that genetic deletion or pharmacological inhibition of HCN1 in degenerating photoreceptors dramatically enhances the disease progression suggesting that HCN1 is an important factor that counteracts degeneration of photoreceptors.

For Peer Review

Results

Loss of *Hcn1* enhances photoreceptor degeneration in *Cngb1* knockout (KO) mice.

To test whether HCN1 influences the function and structure of degenerating rod photoreceptors, we cross-bred *Hcn1* KO mice with the *Cngb1* KO mouse model of retinitis pigmentosa (22) to obtain *Cngb1* x *Hcn1* double KO (*Cngb1*/*Hcn1* DKO) mice. We first performed ERG measurements to assess the effect of HCN1 deletion on the photoresponse in *Cngb1* KO mice. We recorded both scotopic and photopic ERGs in 4-month-old *Cngb1*/*Hcn1* DKO mice and found an almost complete loss of rod- and cone-driven responses (Figure 1A). This result was quite surprising since we had previously shown that, although a deletion of *Cngb1* strongly impairs the rod-driven scotopic ERG responses, it does not affect cone-driven photopic ERG responses until 6 months of age (22). To further elucidate this inconsistency, we recorded ERGs in 4-week-old *Cngb1*/*Hcn1* DKO and age-matched *Cngb1* KO control mice. As shown in Figure 1B, both rod- and cone-driven responses were present in 4-week-old *Cngb1*/*Hcn1* DKO mice, but amplitudes were smaller than those in 4-week-old *Cngb1* KO control mice (Figure 1B-C). These findings suggest a faster or exacerbated photoreceptor degeneration in the absence of HCN1. This phenomenon was investigated further at the level of retinal morphology. First, we examined the morphology of rod and cone photoreceptors in the retinas of 90-day-old *Cngb1*/*Hcn1* DKO mice. We labeled retinal cross sections with a peripherin-2 (Prph2) specific antibody to reveal rod morphology and peanut agglutinin (PNA) to mark cones. Both markers had a similar appearance in wild type and *Hcn1* KO mice (Figure 2A) confirming that HCN1 channel deletion alone has no effect on photoreceptor morphology. In 90-day-old *Cngb1* KO mice both morphological markers were preserved (Figure 2A). However, some signs of a moderate degeneration were already evident, including a reduction in both rod outer segment length and photoreceptor nuclear layer thickness (Figure 2A and (22)). In striking contrast, the photoreceptor layer in *Cngb1*/*Hcn1*

For Peer Review

DKO mice of the same age was already reduced to only 1-2 rows, and rod and cone cell markers were barely preserved (Figure 2A). In comparison, the retina of a 28-day-old *Cngb1*/*Hcn1* DKO showed great similarity with that of a 90-day-old *Cngb1* KO mouse (Figure 2A).

To characterize the time course of degeneration, we applied optical coherence tomography (OCT), a powerful imaging technique that generates virtual cross sections through tissues and enables the visualization and quantification of retinal layer thickness (Figure 2B) *in vivo* (23). We started imaging wild type, *Cngb1* KO and *Cngb1*/*Hcn1* DKO mice right after eye opening (day 14) and followed them up to 5 months of age. At postnatal day 14, the gross retinal layer morphology was similar in all three genotypes (Figure 2B-C). In wild type mice, the photoreceptor layer thickness did not substantially change over the observation period (Figure 2C). At 5 months of age, the photoreceptor layer thickness in *Cngb1* KO mice had decreased by almost one half to 49.50 ± 1.31 µm (n = 6) (Figure 2C). In *Cngb1*/*Hcn1* DKO mice, the disease progression was significantly faster (Figure 2C). Three months after birth, the photoreceptor layer in the double knockout was so much reduced that it could no longer be resolved by OCT (Figure 2B). In contrast, deletion of *Hcn1* alone had no negative effect on retinal morphology and photoreceptor layer thickness (Figure S1). Accordingly, the thickness of the photoreceptor layer in aged Hcn1 KO retina (100.2 ± 2.0 µm, n = 6) was similar to wild type (101.8 ± 1.6, n = 6; Figure S1). The examination of the ocular fundus using confocal laser scanning ophthalmoscopy (cSLO) confirmed the observed changes in 5 month old *Cngb1*/*Hcn1* DKO mice and revealed a marked atrophy of the retinal pigment epithelium (RPE), which was not observed in wild type or *Cngb1* KO mice (Figure 2D).

Taken together, these findings point to a context-specific deleterious effect of a genetic deletion of *Hcn1* on retinal morphology in the *Cngb1* KO mouse model of RP. This effect manifests as an enhanced degeneration of rod photoreceptors, associated with an accelerated secondary degeneration of cone photoreceptors and RPE cells.

For Peer Review

Pharmacological inhibition of I_h enhances photoreceptor degeneration in *Cngb1* KO mice.

To test if the disease amplifying effect resulted specifically from the lack of HCN channel function we treated *Cngb1* KO mice with the I_h current blocker zatebradine and analyzed the progression of photoreceptor degeneration using OCT. Wild type and *Cngb1* KO mice received daily i.p. injections of zatebradine (10 µg / g body weight / day) or vehicle for ten consecutive days starting on postnatal day 11.The retinal thickness was then assessed at day 21, 60 and 90 (Figure 3A). Confirming the morphological data from *Hcn1* KO mice (Figures 2A and S1), there was no sign of retinal thinning in zatebradine-treated wild type mice (Figure 3B-C). Moreover, zatebradine had no short-term effects on the *Cngb1* KO retina since the photoreceptor layer thickness was similar in treated and untreated KO mice at the end of the 10 day treatment period (Figure 3C). However, at 40 and 70 days after zatebradine treatment we observed a significant reduction of the photoreceptor layer thickness in *Cngb1 KO* mice (Figure 3B-C; 2-way-ANOVA, $p < 0.001$), supporting the view that loss of HCN1 channel function in rod photoreceptors enhances the disease progression in the *Cngb1* KO mouse model of RP.

Adeno-associated viral (AAV) vectors-mediated expression of HCN1 in *Cngb1*/*Hcn1* DKO mice rescues photoreceptors from enhanced degeneration.

To confirm that HCN1 function in rods is crucial for survival of *Cngb1*-deficient rod photoreceptors, we generated recombinant AAVs expressing the mouse HCN1 channel as a N-terminal YFP-fusion protein under control of the rod photoreceptor-specific rhodopsin promoter and delivered them into the subretinal space of 14-day-old *Cngb1*/*Hcn1* DKO mice. YFP fluorescence, indicative for the YFP-HCN1 channel expression, became detectable seven days post injection in the treated part of the retina (data not shown). Importantly, 4 weeks

For Peer Review

later the treated (fluorescent) part of the *Cngb1*/*Hcn1* DKO retina was substantially better preserved compared to the untreated (non-fluorescent) part (Figure 3D). In contrast to the untreated part, the photoreceptor layer in the treated part still contained 4-6 rows of photoreceptors (Figure 3D).

Effect on *Hcn1* deletion on the photovoltage of degenerating rods.

In healthy photoreceptors, HCN1 channels open in response to light-evoked hyperpolarization and contribute to shaping the photovoltage (12-14). Our results so far suggested that the disease-amplifying effect in degenerating *Cngb1*/*Hcn1* DKO rod photoreceptors can be attributed to the missing function of the HCN1 channels. This prompted us to determine the range of membrane potentials in which mutant rods operate. To this end, we used a previously described perforated patch recording technique to current- or voltage-clamp rod photoreceptors in mouse retinal slices (24). As an important initial experiment, we compared wild type and *Hcn1* KO rod photoreceptors (Figure S2). The mean dark membrane potential (V_{dark}) in adult wild type rods was -35.4 ± 1.6 mV (mean ± SEM, n = 19). *Hcn1* KO rods had similar V_{dark} values at -34.1 ± 2.0 mV (n = 4), confirming that HCN1 does not significantly contribute to the dark membrane potential of rod photoreceptors. Moreover, saturating light stimuli resulted in similar levels of hyperpolarization in wild type 55.4 ± 2.2 mV (n =19) and *Hcn1* KO rods 54.2 ± 2.6 mV (n =4).

To test whether HCN1 influences the electrical properties of degenerating rod photoreceptors, we next compared wild type, *Cngb1* KO, and *Cngb1/Hcn1* DKO rod photoreceptors. To exclude measuring end stage degenerating photoreceptors, we performed the experiments on retinal slices from 15 to 20-day-old mice, which is prior to the peak of rod degeneration in *Cngb1* KO mice (22, 25). As expected I_h was present in wild type and *Cngb1* KO rods, but absent in DKO rods (Figure 4A) confirming that HCN1 is the major HCN channel isoform in rod photoreceptors. Rod photoreceptors in young wild type mice had a mean V_{dark} of -37.9 ±

For Peer Review

1.1 mV (n = 5) (Figure 4B). Although the V_{dark} of *Cngb1* KO rods (-34.9 ± 0.9 mV, n = 14) was slightly more depolarized than in wild type rods, there was no statistically significant difference between the groups (1-way ANOVA) (Figure 4B). Additional deletion of HCN1 in *Cngb1* KO mice did not change V_{dark} significantly (-36.4 ± 1.0 mV, n = 8) (Figure 4B), arguing against a major role of HCN1 in setting the dark membrane potential in degenerating rods. Short light (flash) stimuli cause a fast hyperpolarization of the mouse rod photovoltage, which returns to the V_{dark} after a few seconds (24). The response of young wild type rods to flash stimuli of varying intensities is shown in Figure 4C. In wild type rods the saturating flash stimulus caused a maximal hyperpolarization of about 15 mV in amplitude to -53.4 ± 2.5 mV (n = 5) (Figure 4B). In line with the previously reported suction pipette recordings from rod outer segments (22), the light responses in *Cngb1* KO rods were strongly compromised: saturating flash stimuli only weakly hyperpolarized *Cngb1* KO rods to -37.7 ± 1.5 mV (n = 14) (Figure 4B). Similarly, in *Cngb1*/*Hcn1* DKO rods the bright flash resulted only in a minor peak hyperpolarization to -37.7 ± 1.4 mV (n = 8) (Figure 4B). The rare *Cngb1* KO and *Cngb1*/*Hcn1* DKO rods that showed a flash response displayed a greatly reduced amplitude, slower onset and recovery kinetics and a less pronounced "nose" (13) compared to the wild type rods (Figure 4C).

In the absence of *Cngb1*, only small amounts of homotetrameric CNGA1 channels are present in rod outer segments (22). Given that the dark current is mediated by CNG channels (26), the smaller number of functional CNG channels should have led, other factors being equal, to a more hyperpolarized dark membrane potential. The finding that the actual measured V_{dark} in *Cngb1* KO and *Cngb1/Hcn1* DKO rods was not significantly different from wild type suggests that unidentified conductances result in a constitutive depolarization of *Cngb1*-deficient rods. To test this hypothesis, we analyzed the peak membrane potential reached in response to a saturating flash (V_{dark} – max flash response), since saturating light eliminates the contribution of the dark current. In line with this idea, both *Cngb1* KO and *Cngb1/Hcn1* DKO

For Peer Review

rods were significantly depolarized relative to wild type rods (1-way ANOVA, P<0.0001), while no significant difference was detected between the two mutants (Figure 4B).

Taken together, these data indicate that the protective role of HCN1 channels during the early stages of photoreceptor degeneration cannot be attributed to a straightforward effect on cellular membrane potential. In fact, we found that juvenile *Cngb1* KO rods are in a constitutively depolarized state.

Involvement of Ca^{2+} and calpain in photoreceptor degeneration in *Cngb1/Hcn1* DKO mice.

To investigate if impaired Ca^{2+} signaling is involved in the accelerated disease progression of *Cngb1*/*Hcn1* DKO mice, we analyzed the levels of calpain activation using an *in situ* activity assay. Calpain is a Ca^{2+}-dependent protease involved in neuronal and photoreceptor cell death (27, 28). Calpain activity was found to be elevated in a subset of photoreceptors in *Cngb1* KO mice (25). Here, we found that in *Cngb1*/*Hcn1* DKO mice significantly more photoreceptors showed elevated calpain activity compared to *Cngb1* single KO mice (Figure 5A-B).

The main gates for calcium entry into photoreceptors are the outer segment plasma membrane CNG channel and the synaptic voltage-gated calcium channel (VGCC). Since the CNG channel composition and expression is strongly impaired by the *Cngb1* deletion (22), a contribution of any potentially existing small amounts of residual CNG channels to the Ca^{2+} elevation is unlikely. To test for the contribution of the VGCC, we cross-bred the *Cngb1*/*Hcn1* DKO mice with *Cacna1f* knockout mice lacking expression of the $Ca_v1.4$ $\alpha1$ subunit of the VGCC channel (29, 30) and compared the development of photoreceptor layer thinning in these triple knockout (TKO) mice to that in the *Cngb1*/*Hcn1* DKO mouse. Indeed, in *Cngb1*/*Hcn1*/*Cacna1f* TKO mice the thinning of the photoreceptor layer progressed significantly slower compared to *Cngb1*/*Hcn1* DKO mice (Figure 5C-D) (2-way ANOVA, $p < 0.01$). However, the disease progression was not halted and still progressed faster than in

For Peer Review

Cngb1 KO mice suggesting that additional Ca^{2+} sources contribute to the effect. Given that deletion of *Cacna1f* alone does not result in rod photoreceptor degeneration itself (30), the residual CNG channel and/or unknown calcium sources might contribute to the activation of calpain.

Effect of HCN1 deletion on cone photoreceptor degeneration.

HCN1 is expressed in both types of photoreceptors, rods and cones (14). Thus, the neuroprotective mechanism of HCN1 in degenerating rods might also be relevant for degenerative cone photoreceptor diseases. To test if deletion of HCN1 exerts a similar disease-amplifying effect in cone degeneration, we cross-bred *Hcn1* KO mice with the *Cnga3* KO mouse model of achromatopsia (1). Cone photoreceptor degeneration in *Cnga3* KO mice progresses slowly in the superior (dorsal) part of the retina and rather fast in the inferior (ventral) retina (31). Accordingly, at 3 months of age the cone density is significantly lower in the ventral compared to the dorsal part of the *Cnga3* KO retina, resulting in areas with distinct levels of disease progression. We compared the cone photoreceptor density in 3-month-old *Cnga3* KO with age-matched *Cnga3/Hcn1* DKO mice, and found that loss of *Hcn1* significantly reduced the number of surviving cone photoreceptors by 1.5 fold in the dorsal and by 10 fold in the ventral part of the *Cnga3*-deficient retina (Figure 6A-B, Figure S3). Thus, the neuroprotective effect of HCN1 is not only restricted to rod photoreceptors, but also applies to diseases with cell-autonomous cone photoreceptor degeneration.

For Peer Review

Discussion

HCN1 is a highly abundant photoreceptor inner segment plasma membrane ion channel (10, 14) involved in shaping the rod and cone photoresponses (12-14). In particular, studies in *Hcn1* KO mice revealed that lack of HCN1 prolongs the rod photoresponse (14), which in turn inhibits cone signaling under mesopic conditions (15). Pharmacological inhibition of HCN channels also affects retinal function. Patients treated with the I_h blocker ivabradine report the occurrence of phosphenes (19, 20) and ERG measurements in animal models demonstrated a modulation of the photoresponse after pharmacological HCN inhibition (32, 33). However, no reports exist linking pharmacological inhibition of I_h or a genetic deficiency of *HCN1* with photoreceptor degeneration.

In this study, we analyzed the effect of HCN1 on the viability of degenerating rod or cone photoreceptors. We show that the genetic ablation of *Hcn1* or systemic administration of the I_h blocker zatebradine both exacerbate degeneration and loss of rod photoreceptors in the *Cngb1* KO mouse model of RP. A similar deleterious effect on cone viability was observed after genetic deletion of *Hcn1* in the *Cnga3* KO mouse model of achromatopsia. Genetic deletion of *Hcn1* alone, however, had no effect on the retinal morphology and photoreceptor survival. Based on these findings, we propose that HCN1 function serves a neuroprotective role in inherited retinal diseases with a primary defect in rod or cone photoreceptors like RP or achromatopsia.

A previous study by Della Santina et al. (17) addressed the effects of the I_h blocker ivabradine on the progression of retinal degeneration in the *rd10* mouse model of RP. The study was designed to analyze the acute and short-term (up to 3 weeks) effects of systemic ivabradine administration on retinal function and morphology. The authors found no effect of ivabradine on photoreceptor degeneration in the *rd10* mice during a 3 week observation period. In line with Della Santina et al. (17), we also did not observe any short-term effects of I_h inhibition

For Peer Review

on retinal morphology in our study. However, when examining longer term effects at 7 or approx. 11 weeks after treatment, we found that inhibition of I_h resulted in enhanced thinning of the photoreceptor layer in the *Cngb1* KO mouse model of RP. In addition to the different observation periods, the two studies used distinct I_h blockers (ivabradine vs zatebradine) but with similar potency on HCN channels (34). We cannot exclude that factors other than the observation period and the type of I_h blocker might have contributed to the different outcome. One additional factor may be the use of differing mouse models of RP. In particular, the lack of PDE6B function in the *rd10* mouse (35, 36) analyzed in Della Santina et al. (17) results in a much more rapid photoreceptor degeneration than the lack of CNGB1 in the *Cngb1* KO mouse model (22) utilized in our study. Given the relatively fast disease progression in the *rd10* mouse, it might be more difficult to detect an enhancement of photoreceptor degeneration by inhibition of I_h than in the slow degenerating *Cngb1* KO retina.

Mechanistically, loss of HCN1 function leads to increased activation of the Ca^{2+}-dependent protease calpain, which is known to be involved in cell death in many mouse models of photoreceptor degeneration (25). It appears that the Ca^{2+}/calpain effect depends at least partially on the presence of the synaptic voltage-gated calcium channels Cav1.4 (*Cacna1f*). The role of other Ca^{2+} sources in this regard is still unclear. However, a major contribution of the CNG channel can be excluded in both mouse models analyzed in this study (*Cngb1* KO and *Cnga3* KO).

In summary, we show here a protective effect of HCN1 channels on photoreceptor degeneration on the basis of both pharmacological data and genetic inactivation studies in murine models of RP and achromatopsia. Together, these data strongly support the view that HCN1 is a major factor for outer retinal viability in primary photoreceptor diseases.

The HCN inhibitor ivabradine is clinically used for the treatment of stable angina pectoris or heart failure. In the light of these findings, it may be recommended to reevaluate whether I_h

For Peer Review

blockers might be harmful to the eyesight in patients suffering from retinal degenerative disorders.

For Peer Review

Materials and Methods

Animals

Hcn1 KO mice (B6;129-Hcn1^{tm2Knd1}/J, stock number #005034, The Jackson Laboratory) (37) were cross-bred with mice lacking either *Cngb1* (22) or *Cnga3* (1) to generate *Cngb1/Hcn1* and *Cnga3/Hcn1* DKO mice, respectively. To obtain *Cngb1/Hcn1/Cacna1f* TKO mice, *Cngb1/Hcn1* DKO mice were crossed with a *Cacna1f*-deficient line obtained from Dr. Marion Maw, University of Otago, Dunedin, New Zealand (29, 30). Control experiments were conducted on mice with the same genetic background. All procedures concerning animals were performed with permission of local authorities (Regierung von Oberbayern, Regierungspräsidium Tübingen and Ethical Committee of the University of Pisa) and in accordance with the ARVO Statement for the Use of Animals in Ophthalmic and Vision Research.

Ophthalmologic examinations

For ophthalmologic examinations, adult mice received intraperitoneal injections of ketamin (0.1 mg/g) and xylazin (0.02 mg/g). For mice younger than 3 weeks a lower dose of ketamine (0.05 mg/g) and xylazin (0.01 mg/g) was used. Before the scanning procedure, Tropicamid eye drops were applied to the mice eyes for pupil dilation (Mydriadicum Stulln, Pharma Stulln GmbH, Stulln, Germany). Subsequently, hydroxylpropyl methylcellulose (Methocel 2%; OmniVision, Puchheim, Germany) was applied to keep the eyes moist. The examination was performed with an adapted Spectralis HRA + OCT system from Heidelberg Engineering (Dossenheim, Germany) in combination with optic lenses described previously (38). The system allowed for imaging of the eye fundus by cSLO und examination of the retinal morphology by OCT.

For Peer Review

OCT scans were conducted with a 12° circular scan mode centered at the optic nerve head. This procedure enabled measurements of the photoreceptor layer thickness at a comparable distance from the optic nerve head and allowed for comparison of values in longitudinal examinations of the same eye and between individuals. In detail, photoreceptor layer thickness was measured between the clearly visible outer plexiform layer and the border of neuronal retina and the RPE. For statistical analysis, the mean photoreceptor layer thickness was calculated from single values measured in the dorsal, temporal, nasal and ventral region around the optic nerve. cSLO images of the eye fundus were obtained using the infrared laser (820 nm) and the scanner set to a 30° field of view at high resolution mode.

Pharmacological treatment

In general, pharmacological experiments were conducted on littermates. For the pharmacologic inhibition of HCN channels, mice received a daily injection of 10 mg/kg Zatebradine (Z0127, Sigma-Aldrich) dissolved in 0.9 % NaCl. Littermate controls received a daily injection of 0.9 % NaCl.

Production and *in vivo* application of AAV vectors

Cloning was performed by standard techniques. All sequence manipulations were confirmed by sequencing. The YFP sequence was fused with a glycine-serine-glycine linker to the N-terminus of mouse HCN1 using overlap PCR (39) and ligated with the human rhodopsin promoter sequence (40) into pAAV2.1-MCS (41) to generate pAAV2.1-RHO-YFP-HCN1-WPRE. Single-strand AAV vectors were produced by triple calcium phosphate transfection of HEK 293T cells with pAdDeltaF6 (42), pAAV2/8 Y733F (43), and pAAV2.1-RHO-YFP-HCN1-WPRE plasmids followed by iodixanol-gradient purification of cell lysates after 48 hours (44). The 40–60% iodixanol interface was further purified and concentrated by ion exchange chromatography on a 5 ml HiTrap Q Sepharose column using an ÄKTA Basic

For Peer Review

FPLC system (GE Healthcare, Munich, Germany) followed by further concentration using Amicon Ultra-4 Centrifugal Filter Units (Millipore, Schwalbach, Germany). Physical titers (in vector genome copies/µl) were determined by qPCR with primers specific for the WPRE sequence (41).

Subretinal injections were performed as described previously (45). In brief, anesthetized mice received one microliter containing 7 x 10^8 AAV genomic particles injected into the subretinal space. Special care was taken to avoid damage of the lens. The success of the procedure was monitored immediately following the injections using cSLO and OCT.

Immunohistochemistry

Vertical cryosections (10 µm) of the mouse retina were prepared for immunohistochemical staining as described previously (31). A mouse anti-peripherin-2 monoclonal antibody (mAB 2B7) (46) was applied (at 1:1000 dilution) for labeling of rod photoreceptor outer segments. Cone photoreceptors were stained with a guinea pig anti-glycogen phosphorylase (Glypho) polyclonal antibody ((47); 1:1000) and with fluorescein isothiocyanate conjugated peanut agglutinin (FITC-PNA; 1:100, Sigma-Aldrich). Confocal images were collected on a LSM 510 (Carl Zeiss, Oberkochen, Germany) or a TCS SP8 (Leica, Wetzlar, Germany) microscope.

Calpain activity assay

For detection of calpain activity we performed an *in situ* enzymatic assay on unfixed retinal cryo-sections (48). In detail, sections were covered for 15 min with calpain reaction buffer (CRB: 25 mM HEPES, 65 mM KCl, 2 mM MgCl2, 1.5 mM CaCl2, 2 mM DTT, pH 7.2). Subsequently, 20 µM of the fluorescent calpain substrate 7-amino-4-chloromethylcoumarin, t-BOC-Leucyl-L-methionine amide (Molecular Probes) dissolved in 1% DMSO and 99 % CRB Buffer were added. After an incubation of 1 h 30 min at 37 °C slices were washed 3 x 10 min

For Peer Review

with CRB. Cells with increased calpain activity could be clearly identified due to the fluorescence of the cleaved substrate. Confocal images were obtained using a Zeiss LSM510 at 364 nm excitation (detection LP 385).

Electroretinography

ERG analysis was performed according to procedures described previously (49, 50). In short, single-flash ERG responses were obtained under dark-adapted (scotopic; no background illumination: 0 cd/m^2) and light-adapted (photopic; 30 cd/m^2, starting 10 min before recording) conditions. Single white-flash stimuli ranged from -4 to 1.5 log cd*s/m^2 stimulus intensities under dark-adapted conditions, and from -2 to 1.5 log cd*s/m^2 under light-adapted conditions. Ten responses were averaged with interstimulus intervals of 5 s (for -4to -0.5 log cd*s/m^2) or 17 s (for 0 to 1.5 log cd*s/m^2).

Patch clamp recordings

Current- and voltage-clamp perforated patch clamp recordings of rod photoreceptors in mouse retinal slices were performed as previously described (24, 51). All procedures were approved by the Ethical Committee of the University of Pisa (prot. n. 2891/12) and were conducted in accordance with Italian (D.lgs.vo 116/92) and EU regulations (Council Directive 86/609/EEC). Briefly, juvenile (P15–20) or adult (> P30) mice (see above for strain details) were anaesthetized, their retinas extracted in ice cold AMES' medium (A1420; Sigma-Aldrich, St. Louis, MO, USA), made to adhere on filter paper and sliced on a manual tissue chopper at a thickness of 250 μm. After being transferred in the recording chamber they were superfused at a temperature of ~24 C with bicarbonate-buffered AMES' and visualized with a DIC infrared microscope. Seals were obtained on rod somata with perforated patch pipettes filled with a solution containing (in mM): 90 potassium aspartate, 20 K_2SO_4, 15 KCl, 10 NaCl, 5 K_2Pipes, and 0.4 mg/ml Amphotericin-B. Final pH was set at 7.2 with HCl / KOH.

For Peer Review

Based on the expected liquid junction and Donnan potentials in our recording conditions (24), we report uncorrected values of the membrane potential. Full field flashes were delivered with a green LED (OD520; Optodiode Corp., Newbury Park CA) having its emission peak at 520 nm.

Statistical analysis

Statistical analysis was performed using Graph Pad Prism 5 software. To compare two or more groups at one time point, unpaired Student's t-test or one-way ANOVA tests were applied, respectively. For comparing groups in longitudinal examinations, 2-way ANOVA with Bonferroni post-tests were performed. Unless otherwise stated, all values are given as mean ± SE.

For Peer Review

Funding

This work was supported by the Deutsche Forschungsgemeinschaft (DFG).

Acknowledgements

We thank Gudrun Utz, Pia Lacroix, Jennifer Schmidt and Elisabeth Schulze for excellent technical help, Dr. Marion Maw (University of Otago, Dunedin, New Zealand) for providing the Cacna1f-deficient mouse line, Drs. James M. Wilson (Univ Pennsylvania) and Alberto Auricchio (TIGEM) for the gift of AAV plasmids and Drs. Muna Naash (Oklahoma State Univ) and Brigitte Pfeiffer-Guglielmi (Univ Tübingen) for the gift of antibodies.

Conflict of interest statement

None declared.

For Peer Review

References

1 Biel, M., Seeliger, M., Pfeifer, A., Kohler, K., Gerstner, A., Ludwig, A., Jaissle, G., Fauser, S., Zrenner, E. and Hofmann, F. (1999) Selective loss of cone function in mice lacking the cyclic nucleotide-gated channel CNG3. *Proceedings of the National Academy of Sciences of the United States of America*, **96**, 7553-7557.

2 Biel, M. and Michalakis, S. (2007) Function and dysfunction of CNG channels: insights from channelopathies and mouse models. *Molecular neurobiology*, **35**, 266-277.

3 Cuenca, N., Fernandez-Sanchez, L., Campello, L., Maneu, V., De la Villa, P., Lax, P. and Pinilla, I. (2014) Cellular responses following retinal injuries and therapeutic approaches for neurodegenerative diseases. *Progress in retinal and eye research*, **43**, 17-75.

4 Veleri, S., Lazar, C.H., Chang, B., Sieving, P.A., Banin, E. and Swaroop, A. (2015) Biology and therapy of inherited retinal degenerative disease: insights from mouse models. *Disease models & mechanisms*, **8**, 109-129.

5 Biel, M. and Michalakis, S. (2009) Cyclic nucleotide-gated channels. *Handbook of experimental pharmacology*, in press., 111-136.

6 Burns, M.E. and Baylor, D.A. (2001) Activation, deactivation, and adaptation in vertebrate photoreceptor cells. *Annual review of neuroscience*, **24**, 779-805.

7 Demontis, G.C., Longoni, B., Barcaro, U. and Cervetto, L. (1999) Properties and functional roles of hyperpolarization-gated currents in guinea-pig retinal rods. *The Journal of physiology*, **515 (Pt 3)**, 813-828.

8 Barrow, A.J. and Wu, S.M. (2009) Complementary conductance changes by IKx and Ih contribute to membrane impedance stability during the rod light response. *Channels*, **3**, 301-307.

9 Biel, M., Wahl-Schott, C., Michalakis, S. and Zong, X. (2009) Hyperpolarization-activated cation channels: from genes to function. *Physiological reviews*, **89**, 847-885.

10 Müller, F., Scholten, A., Ivanova, E., Haverkamp, S., Kremmer, E. and Kaupp, U.B. (2003) HCN channels are expressed differentially in retinal bipolar cells and concentrated at synaptic terminals. *The European journal of neuroscience*, **17**, 2084-2096.

11 Gamsiz, E.D., Ouyang, Q., Schmidt, M., Nagpal, S. and Morrow, E.M. (2012) Genome-wide transcriptome analysis in murine neural retina using high-throughput RNA sequencing. *Genomics*, **99**, 44-51.

12 Tanimoto, N., Brombas, A., Muller, F. and Seeliger, M.W. (2012) HCN1 channels significantly shape retinal photoresponses. *Advances in experimental medicine and biology*, **723**, 807-812.

13 Della Santina, L., Piano, I., Cangiano, L., Caputo, A., Ludwig, A., Cervetto, L. and Gargini, C. (2012) Processing of retinal signals in normal and HCN deficient mice. *PloS one*, **7**, e29812.

14 Knop, G.C., Seeliger, M.W., Thiel, F., Mataruga, A., Kaupp, U.B., Friedburg, C., Tanimoto, N. and Müller, F. (2008) Light responses in the mouse retina are prolonged upon targeted deletion of the HCN1 channel gene. *The European journal of neuroscience*, **28**, 2221-2230.

15 Seeliger, M.W., Brombas, A., Weiler, R., Humphries, P., Knop, G., Tanimoto, N. and Müller, F. (2011) Modulation of rod photoreceptor output by HCN1 channels is essential for regular mesopic cone vision. *Nature communications*, **2**, 532.

16 Vinberg, F.J., Strandman, S. and Koskelainen, A. (2009) Origin of the fast negative ERG component from isolated aspartate-treated mouse retina. *Journal of vision*, **9**, 9 1-17.

17 Della Santina, L., Bouly, M., Asta, A., Demontis, G.C., Cervetto, L. and Gargini, C. (2010) Effect of HCN channel inhibition on retinal morphology and function in normal and dystrophic rodents. *Investigative ophthalmology & visual science*, **51**, 1016-1023.

For Peer Review

18 Postea, O. and Biel, M. (2011) Exploring HCN channels as novel drug targets. *Nature reviews. Drug discovery*, **10**, 903-914.
19 Cervetto, L., Demontis, G.C. and Gargini, C. (2007) Cellular mechanisms underlying the pharmacological induction of phosphenes. *British journal of pharmacology*, **150**, 383-390.
20 Riccioni, G. (2012) Ivabradine: an intelligent drug for the treatment of ischemic heart disease. *Molecules*, **17**, 13592-13604.
21 Hartong, D.T., Berson, E.L. and Dryja, T.P. (2006) Retinitis pigmentosa. *Lancet*, **368**, 1795-1809.
22 Hüttl, S., Michalakis, S., Seeliger, M., Luo, D.G., Acar, N., Geiger, H., Hudl, K., Mader, R., Haverkamp, S., Moser, M. *et al.* (2005) Impaired channel targeting and retinal degeneration in mice lacking the cyclic nucleotide-gated channel subunit CNGB1. *The Journal of neuroscience : the official journal of the Society for Neuroscience*, **25**, 130-138.
23 Garcia Garrido, M., Beck, S.C., Mühlfriedel, R., Julien, S., Schraermeyer, U. and Seeliger, M.W. (2014) Towards a quantitative OCT image analysis. *PloS one*, **9**, e100080.
24 Cangiano, L., Asteriti, S., Cervetto, L. and Gargini, C. (2012) The photovoltage of rods and cones in the dark-adapted mouse retina. *The Journal of physiology*, **590**, 3841-3855.
25 Arango-Gonzalez, B., Trifunovic, D., Sahaboglu, A., Kranz, K., Michalakis, S., Farinelli, P., Koch, S., Koch, F., Cottet, S., Janssen-Bienhold, U. *et al.* (2014) Identification of a common non-apoptotic cell death mechanism in hereditary retinal degeneration. *PloS one*, **9**, e112142.
26 Luo, D.G., Xue, T. and Yau, K.W. (2008) How vision begins: an odyssey. *Proceedings of the National Academy of Sciences of the United States of America*, **105**, 9855-9862.
27 Sancho-Pelluz, J., Arango-Gonzalez, B., Kustermann, S., Romero, F.J., van Veen, T., Zrenner, E., Ekstrom, P. and Paquet-Durand, F. (2008) Photoreceptor cell death mechanisms in inherited retinal degeneration. *Molecular neurobiology*, **38**, 253-269.
28 Hara, M.R. and Snyder, S.H. (2007) Cell signaling and neuronal death. *Annual review of pharmacology and toxicology*, **47**, 117-141.
29 Specht, D., Wu, S.B., Turner, P., Dearden, P., Koentgen, F., Wolfrum, U., Maw, M., Brandstatter, J.H. and tom Dieck, S. (2009) Effects of presynaptic mutations on a postsynaptic Cacna1s calcium channel colocalized with mGluR6 at mouse photoreceptor ribbon synapses. *Investigative ophthalmology & visual science*, **50**, 505-515.
30 Michalakis, S., Shaltiel, L., Sothilingam, V., Koch, S., Schludi, V., Krause, S., Zeitz, C., Audo, I., Lancelot, M.E., Hamel, C. *et al.* (2014) Mosaic synaptopathy and functional defects in Cav1.4 heterozygous mice and human carriers of CSNB2. *Hum Mol Genet*, **23**, 1538-1550.
31 Michalakis, S., Geiger, H., Haverkamp, S., Hofmann, F., Gerstner, A. and Biel, M. (2005) Impaired opsin targeting and cone photoreceptor migration in the retina of mice lacking the cyclic nucleotide-gated channel CNGA3. *Investigative ophthalmology & visual science*, **46**, 1516-1524.
32 Gargini, C., Demontis, G.C., Bisti, S. and Cervetto, L. (1999) Effects of blocking the hyperpolarization-activated current (Ih) on the cat electroretinogram. *Vision research*, **39**, 1767-1774.
33 Maccarone, R., Izzizzari, G., Gargini, C., Cervetto, L. and Bisti, S. (2004) The impact of organic inhibitors of the hyperpolarization activated current (Ih) on the electroretinogram (ERG) of rodents. *Archives italiennes de biologie*, **142**, 95-103.
34 Stieber, J., Wieland, K., Stockl, G., Ludwig, A. and Hofmann, F. (2006) Bradycardic and proarrhythmic properties of sinus node inhibitors. *Mol Pharmacol*, **69**, 1328-1337.
35 Gargini, C., Terzibasi, E., Mazzoni, F. and Strettoi, E. (2007) Retinal organization in the retinal degeneration 10 (rd10) mutant mouse: a morphological and ERG study. *The Journal of comparative neurology*, **500**, 222-238.

For Peer Review

36 Chang, B., Hawes, N.L., Hurd, R.E., Davisson, M.T., Nusinowitz, S. and Heckenlively, J.R. (2002) Retinal degeneration mutants in the mouse. *Vision research*, **42**, 517-525.
37 Nolan, M.F., Malleret, G., Lee, K.H., Gibbs, E., Dudman, J.T., Santoro, B., Yin, D., Thompson, R.F., Siegelbaum, S.A., Kandel, E.R. *et al.* (2003) The hyperpolarization-activated HCN1 channel is important for motor learning and neuronal integration by cerebellar Purkinje cells. *Cell*, **115**, 551-564.
38 Schön, C., Hoffmann, N.A., Ochs, S.M., Burgold, S., Filser, S., Steinbach, S., Seeliger, M.W., Arzberger, T., Goedert, M., Kretzschmar, H.A. *et al.* (2012) Long-term in vivo imaging of fibrillar tau in the retina of P301S transgenic mice. *PLoS One*, **7**, e53547.
39 Much, B., Wahl-Schott, C., Zong, X., Schneider, A., Baumann, L., Moosmang, S., Ludwig, A. and Biel, M. (2003) Role of subunit heteromerization and N-linked glycosylation in the formation of functional hyperpolarization-activated cyclic nucleotide-gated channels. *The Journal of biological chemistry*, **278**, 43781-43786.
40 Allocca, M., Mussolino, C., Garcia-Hoyos, M., Sanges, D., Iodice, C., Petrillo, M., Vandenberghe, L.H., Wilson, J.M., Marigo, V., Surace, E.M. *et al.* (2007) Novel adeno-associated virus serotypes efficiently transduce murine photoreceptors. *Journal of virology*, **81**, 11372-11380.
41 Michalakis, S., Mühlfriedel, R., Tanimoto, N., Krishnamoorthy, V., Koch, S., Fischer, M.D., Becirovic, E., Bai, L., Huber, G., Beck, S.C. *et al.* (2010) Restoration of cone vision in the CNGA3-/- mouse model of congenital complete lack of cone photoreceptor function. *Molecular therapy : the journal of the American Society of Gene Therapy*, **18**, 2057-2063.
42 Auricchio, A., Hildinger, M., O'Connor, E., Gao, G.P. and Wilson, J.M. (2001) Isolation of highly infectious and pure adeno-associated virus type 2 vectors with a single-step gravity-flow column. *Hum Gene Ther*, **12**, 71-76.
43 Koch, S., Sothilingam, V., Garcia Garrido, M., Tanimoto, N., Becirovic, E., Koch, F., Seide, C., Beck, S.C., Seeliger, M.W., Biel, M. *et al.* (2012) Gene therapy restores vision and delays degeneration in the CNGB1(-/-) mouse model of retinitis pigmentosa. *Hum Mol Genet*, **21**, 4486-4496.
44 Grieger, J.C., Choi, V.W. and Samulski, R.J. (2006) Production and characterization of adeno-associated viral vectors. *Nat Protoc*, **1**, 1412-1428.
45 Mühlfriedel, R., Michalakis, S., Garcia Garrido, M., Biel, M. and Seeliger, M.W. (2013) Optimized technique for subretinal injections in mice. *Methods Mol Biol*, **935**, 343-349.
46 Chakraborty, D., Conley, S.M., Stuck, M.W. and Naash, M.I. (2010) Differences in RDS trafficking, assembly and function in cones versus rods: insights from studies of C150S-RDS. *Hum Mol Genet*, **19**, 4799-4812.
47 Pfeiffer-Guglielmi, B., Fleckenstein, B., Jung, G. and Hamprecht, B. (2003) Immunocytochemical localization of glycogen phosphorylase isozymes in rat nervous tissues by using isozyme-specific antibodies. *J Neurochem*, **85**, 73-81.
48 Sothilingam, V., Garcia Garrido, M., Jiao, K., Buena-Atienza, E., Sahaboglu, A., Trifunovic, D., Balendran, S., Koepfli, T., Muhlfriedel, R., Schon, C. *et al.* (2015) Retinitis pigmentosa: impact of different Pde6a point mutations on the disease phenotype. *Hum Mol Genet*, in press.
49 Tanimoto, N., Muehlfriedel, R.L., Fischer, M.D., Fahl, E., Humphries, P., Biel, M. and Seeliger, M.W. (2009) Vision tests in the mouse: Functional phenotyping with electroretinography. *Frontiers in bioscience*, **14**, 2730-2737.
50 Seeliger, M.W., Grimm, C., Stahlberg, F., Friedburg, C., Jaissle, G., Zrenner, E., Guo, H., Reme, C.E., Humphries, P., Hofmann, F. *et al.* (2001) New views on RPE65 deficiency: the rod system is the source of vision in a mouse model of Leber congenital amaurosis. *Nature genetics*, **29**, 70-74.

For Peer Review

51 Asteriti, S., Gargini, C. and Cangiano, L. (2014) Mouse rods signal through gap junctions with cones. *eLife*, **3**, e01386.

For Peer Review

Captions to Figures

Figure 1. Knockout of *Hcn1* leads to premature vision loss in *Cngb1*-deficient mice at 4 months. (A) Representative dark-adapted (scotopic, left) and light-adapted (photopic, right) single-flash ERG intensity series of 4-months-old *Cngb1*/*Hcn1* double knockout (DKO) mice (red traces). **(B)** Superimposed representative dark-adapted (scotopic, left) and light-adapted (photopic, right) single-flash ERG intensity series of 4-weeks-old *Cngb1*/*Hcn1* double knockout (DKO) mice (green traces) and *Cngb1* KO mice (black traces). The vertical line indicates the timing of the light stimulus in each panel. **(C)** Box-and-Whisker plots of the b-wave amplitudes plotted as a function of the logarithm of the flash intensity for entire groups: boxes indicate the 25 and 75 % range, the whiskers the 5 and 95 % quantiles, asterisks mark the median of the data.

For Peer Review

Figure 2. Knockout of *Hcn1* enhances photoreceptor degeneration in *Cngb1*-deficient mice. (A) Retinal cryo-sections of wild type, *Hcn1* KO, *Cngb1* KO and *Cngb1*/*Hcn1* DKO mice stained with markers specific for rods (peripherin 2, red) and cones (peanut agglutinin, green). **(B)** Upper part: *In vivo* OCT scan of a wild type retina illustrating the quantification of photoreceptor layer thickness. Lower part: Representative OCT images revealing the progressive photoreceptor layer thinning in *Cngb1* KO and *Cngb1*/*Hcn1* DKO mice. **(C)** Quantification of photoreceptor layer thickness of the different genotypes from 2 weeks to 22 weeks of age. Each data point represents one retina (n = 4-8 per genotype and time point). **(D)** Infrared images of the mouse fundus revealing a severe RPE atrophy in *Cngb1*/*Hcn1* DKO at 5 months of age. onh, optic nerve head; onl, outer nuclear layer; os, outer segments.

For Peer Review

Figure 3. Pharmacologic HCN inhibition accelerates the retinal degeneration of *Cngb1* KO mice. (A) *Cngb1 KO* or wild type mice were treated with the HCN inhibitor zatebradine (P11 - P20, daily 10 µg/g i.p.) or vehicle. Repeated OCT measurements were performed at day 21, 60 and 90. (B) Retinal morphology of treated and non-treated wild type and *Cngb1 KO* mice at day 21 and 90. **(C)** Quantification of photoreceptor layer thickness of treatment groups at day 21, 60 and 90. Each data point represents the mean of photoreceptor layer thickness (n = 4 - 8) ± SEM; ***P < 0.001. **(D)** Overview on a *Cngb1*/*Hcn1* DKO retina (week 6) injected with pAAV2.1-Rho-YFP-HCN1-WPRE at day 14. The AAV-mediated HCN1 expression (indicated by YFP, green) substantially rescued photoreceptor degeneration in the treated part of the retina. gcl, ganglion cell layer; inl, inner nuclear layer; onl, outer nuclear layer. Scale bar in (D) marks 100 µm.

For Peer Review

Figure 4. Knockout of *Hcn1* has no major effect on the membrane potential of depolarized rods in the *Cngb1* KO. (A) Representative families of current traces during hyperpolarizing voltage clamp steps from a holding potential of –53 mV, to –60/–67/–74/–81/–88/–95/–102/ –109 mV, and depolarization to –65 mV (wild type, *Cngb1* KO and *Cngb1* / *Hcn1* DKO rods). **(B)** Box plot showing V_{dark} (shaded box) and V_{dark} – max flash response (empty box) of juvenile wild type, *Cngb1* KO and *Cngb1* / *Hcn1* double KO rods. **(C)** Photovoltage responses to flashes of increasing strength measured in wild type, *Cngb1* KO and *Cngb1*/*Hcn1* DKO rods, respectively (flash strengths in the range of 0.5 – 398 photons/μm^2). Data represented in panel (B) is the median value (thick horizontal line), interquartile range (the box), min and max values (narrow error bars). ** $P<0.001$.

For Peer Review

Figure 5. Involvement of calpain and Cav1.4 in the photoreceptor degeneration of *Cngb1*/*Hcn1* DKO mice. (A) Calpain activity assay performed on unfixed retinal cryo sections of *Cngb1* and *Cngb1*/*Hcn1* DKO mice. **(B)** Quantification of photoreceptors exhibiting calpain activity. Bars represents the mean percentage of photoreceptors with calpain activity (n = 3) ± SEM; ***P < 0.001. **(C)** Representative OCT images of *Cngb1*/*Hcn1* DKO and *Cngb1*/*Hcn1*/*Cacna1f* TKO mice at day 59 revealing the less pronounced thinning of the photoreceptor layer in the absence of Cav1.4 channels. **(D)** Photoreceptor layer thickness of *Cngb1*/*Hcn1* DKO and *Cngb1*/*Hcn1*/*Cacna1f* TKO mice at day 32 and 59. The quantification is based on repeated *in vivo* OCT measurements. Each data point represents the mean photoreceptor layer thickness (n = 5 - 6) ± SEM; **P < 0.01. gcl, ganglion cell layer; inl, inner nuclear layer; onl, outer nuclear layer. Scale bar in (A) marks 25 µm.

For Peer Review

Figure 6. Knockout of *Hcn1* enhances photoreceptor degeneration in *Cnga3*-deficient mice. (**A)** Retinal cryo-sections of *Cnga3* KO and *Cnga3*/*Hcn1* DKO mice stained with two specific markers for cones, glycogen phosphorylase (red) and peanut agglutinin (green). Representative confocal images captured from the dorsal or the ventral part of the retina on cryo-sections through the level of the optic nerve. **(B)** Graph showing the quantification of cone photoreceptor density (cones/mm^2, n = 3) in the dorsal and ventral part as mean ± SEM; **P < 0.01, ***P < 0.001. onl, outer nuclear layer; os, outer segments. Scale bar in (A) marks 25 μm.

For Peer Review

Figure S1. Knockout of *Hcn1* has no major effect on retinal morphology and photoreceptor layer thickness. (A) Representative OCT images from 6-month-old wildtype and *Hcn1* KO mice. **(B)** Graph showing the photoreceptor layer thickness in 6 month old wild type and Hcn1 KO mice measured by optical coherence tomography.

For Peer Review

Figure S2. Knockout of *Hcn1* has no major effect on the membrane potential of rod photoreceptors. Box plot showing V_{dark} (shaded box) and V_{dark} – max flash response (empty box) of adult wild type and *Hcn1* KO rods. Data is the median value (thick horizontal line), interquartile range (the box), min and max values (narrow error bars). ** $P < 0.01$, ** $P < 0.001$.

For Peer Review

Figure S3. Knockout of *Hcn1* enhances photoreceptor degeneration in *Cnga3*-deficient mice. (**A-B)** Representative confocal overview images obtained by stitching of individual 20x images. Retinal cryo-sections of *Cnga3* KO (A) and *Cnga3*/*Hcn1* DKO mice (B) are shown stained with the specific cone marker peanut agglutinin (grey). In addition to cones, peanut agglutinin also labels structures in the inner plexiform layer, the optic nerve head (onh) and blood vessels. Magnified images from the boxed areas are shown as inlays. onl, outer nuclear layer; os, outer segments. The scale bar marks 150 µm.

For Peer Review

Abbreviations

AAV	adeno-associated virus
CRB	Calpain reaction buffer
CNG	cyclic nucleotide-gated channel
cSLO	confocal laser scanning ophthalmoscopy
ERG	electroretinogram
GCL	ganglion cell layer
HCN1	hyperpolarization-activated cyclic nucleotide-gated channel 1
INL	inner nuclear layer
KO	knockout
OCT	optical coherence tomography
ONL	outer nuclear layer
PNA	peanut agglutinin
Prph2	pheripherin-2
RP	retinitis pigmentosa
RPE	retinal pigment epithelium
VGCC	voltage-gated calcium channel

For Peer Review

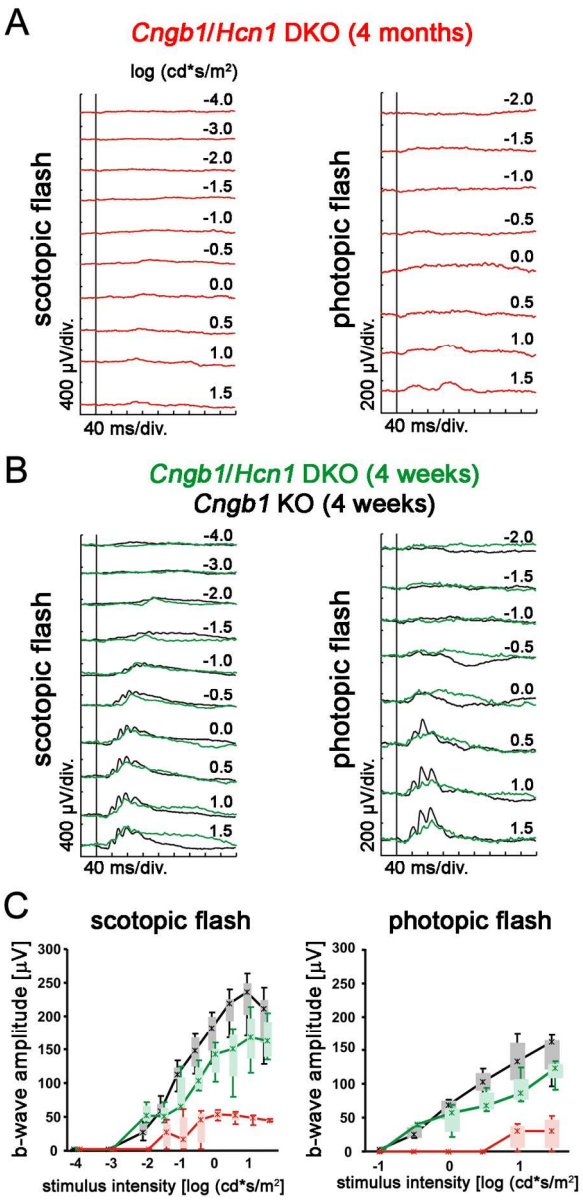

Figure 1. Knockout of Hcn1 leads to premature vision loss in Cngb1-deficient mice at 4 months.
90x186mm (300 x 300 DPI)

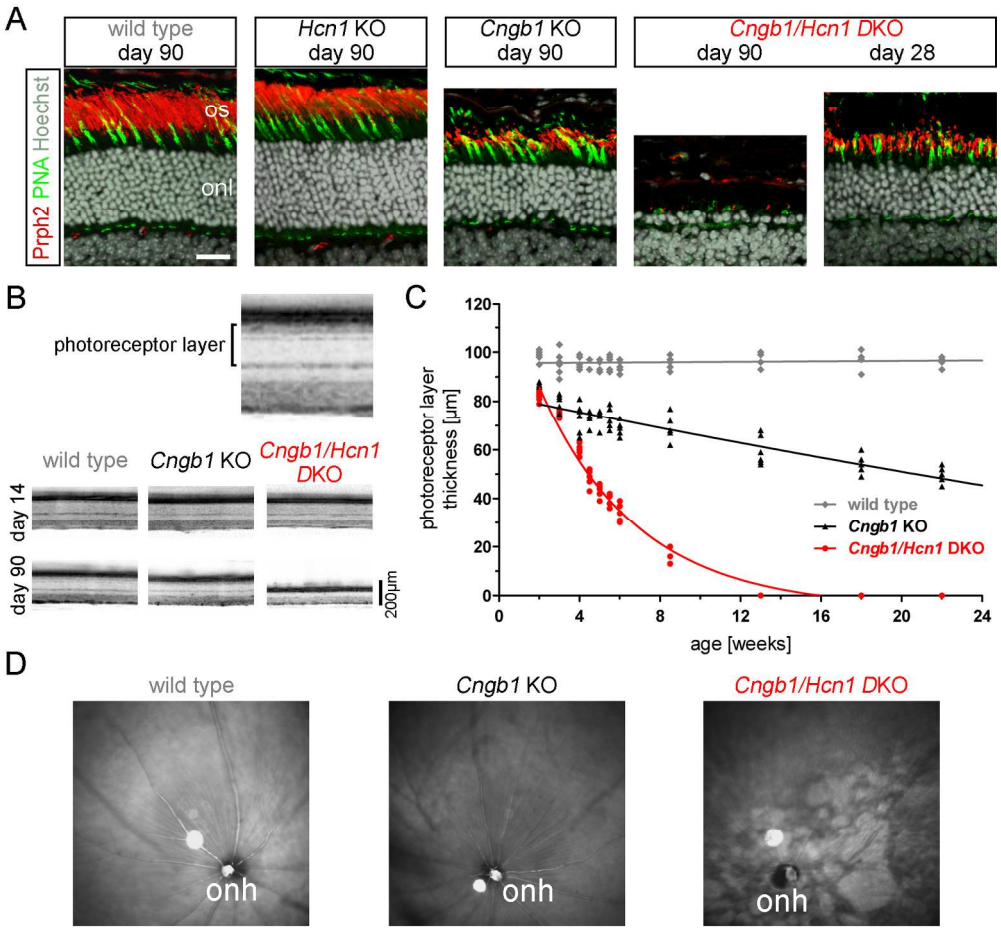

Figure 2. Knockout of Hcn1 enhances photoreceptor degeneration in Cngb1-deficient mice.
177x165mm (300 x 300 DPI)

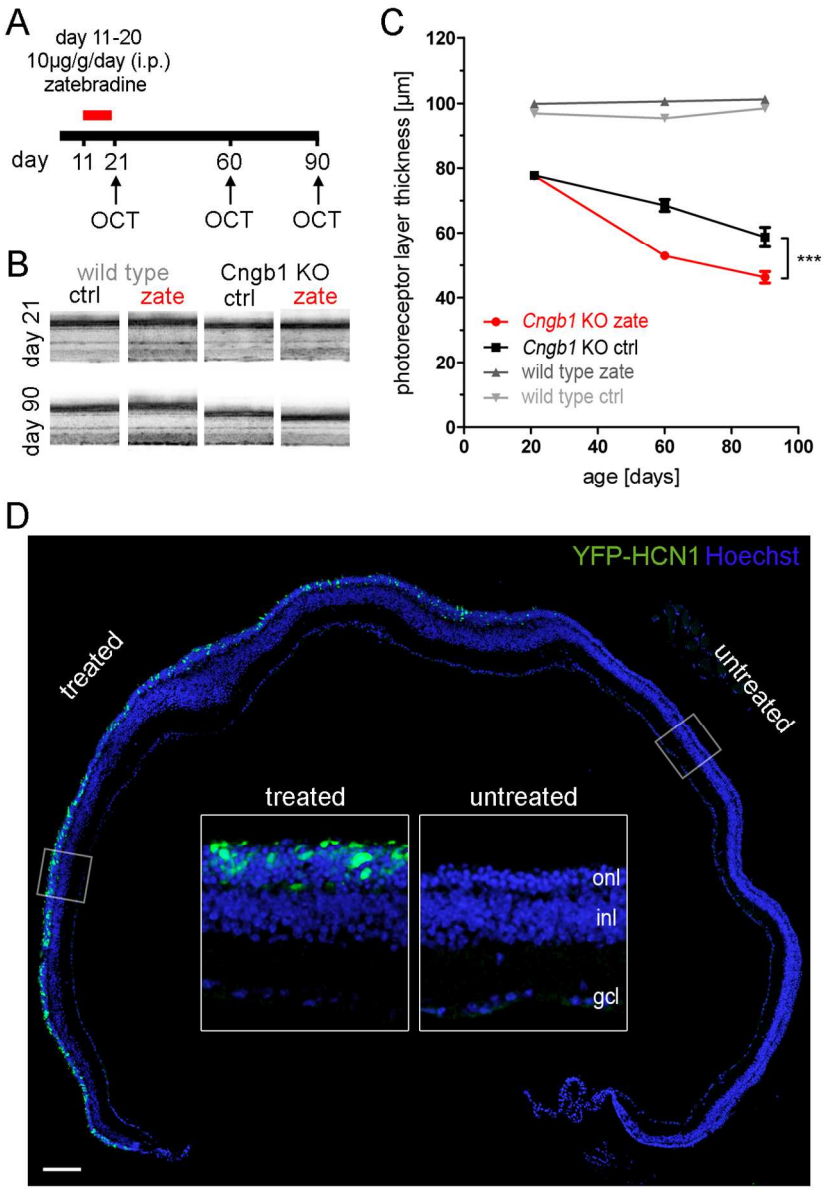

Figure 3. Pharmacologic HCN inhibition accelerates the retinal degeneration of Cngb1 KO mice.
113x163mm (300 x 300 DPI)

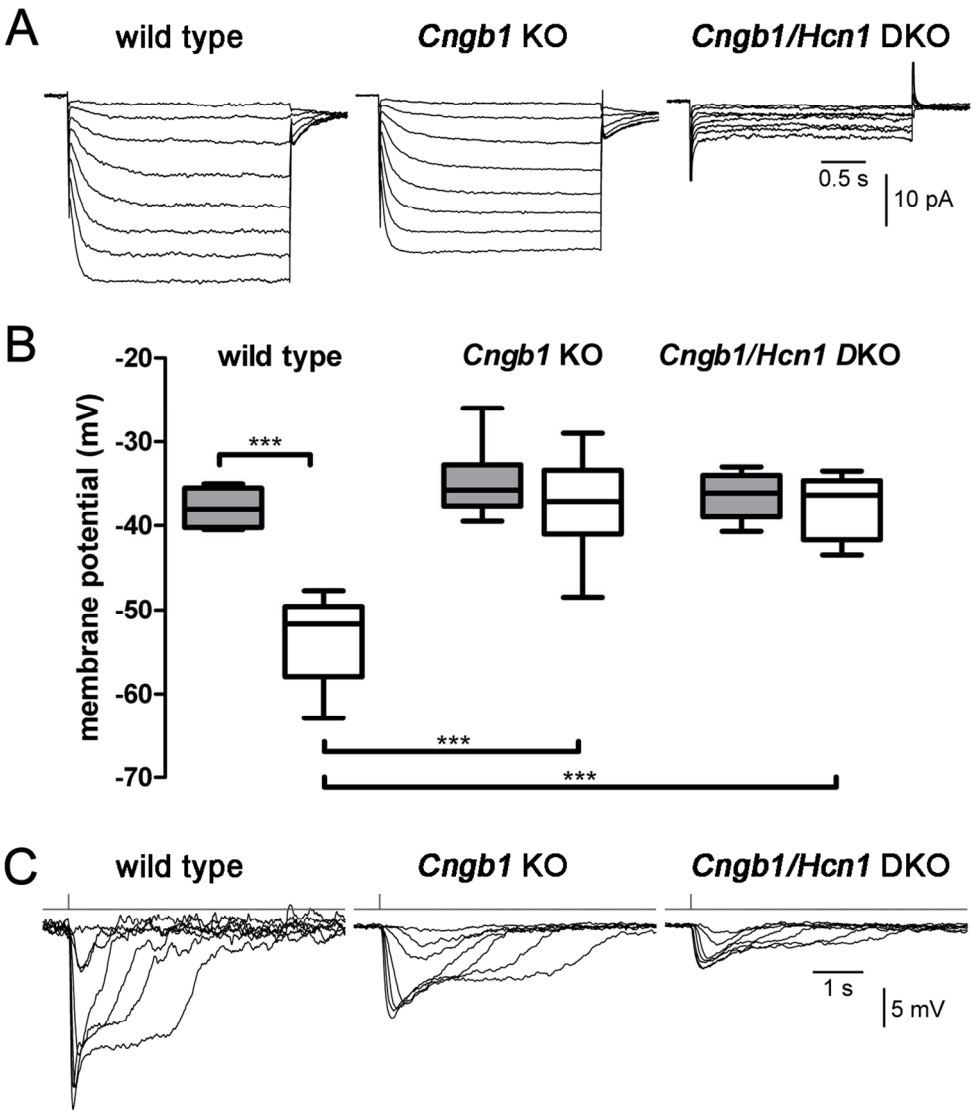

Figure 4. Knockout of Hcn1 has no major effect on the membrane potential of depolarized rods in the Cngb1 KO.
113x127mm (300 x 300 DPI)

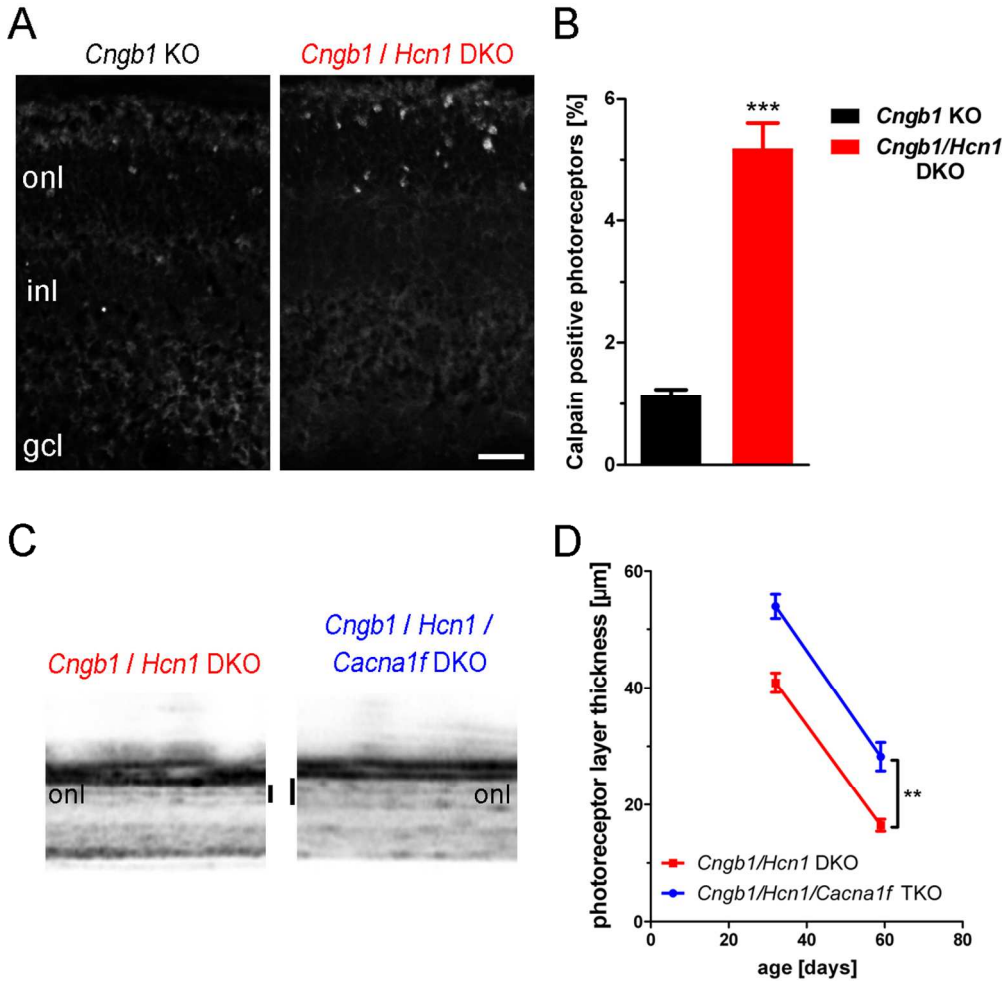

Figure 5. Involvement of calpain and Cav1.4 in the photoreceptor degeneration of Cngb1/Hcn1 DKO mice.
113x111mm (300 x 300 DPI)

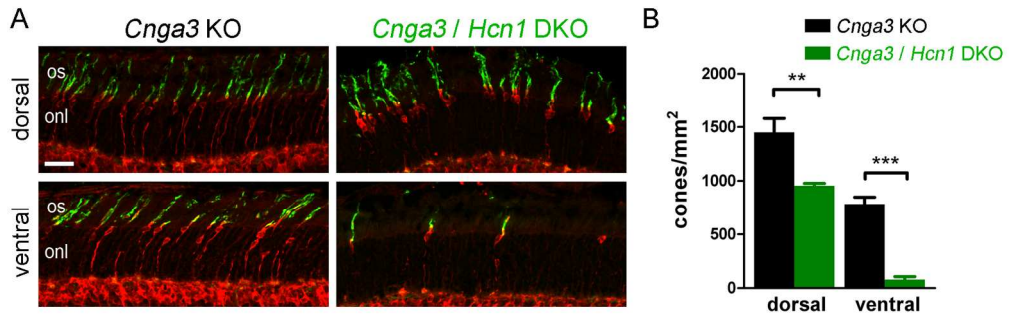

Figure 6. Knockout of Hcn1 enhances photoreceptor degeneration in Cnga3-deficient mice.
180x57mm (300 x 300 DPI)

For Peer Review

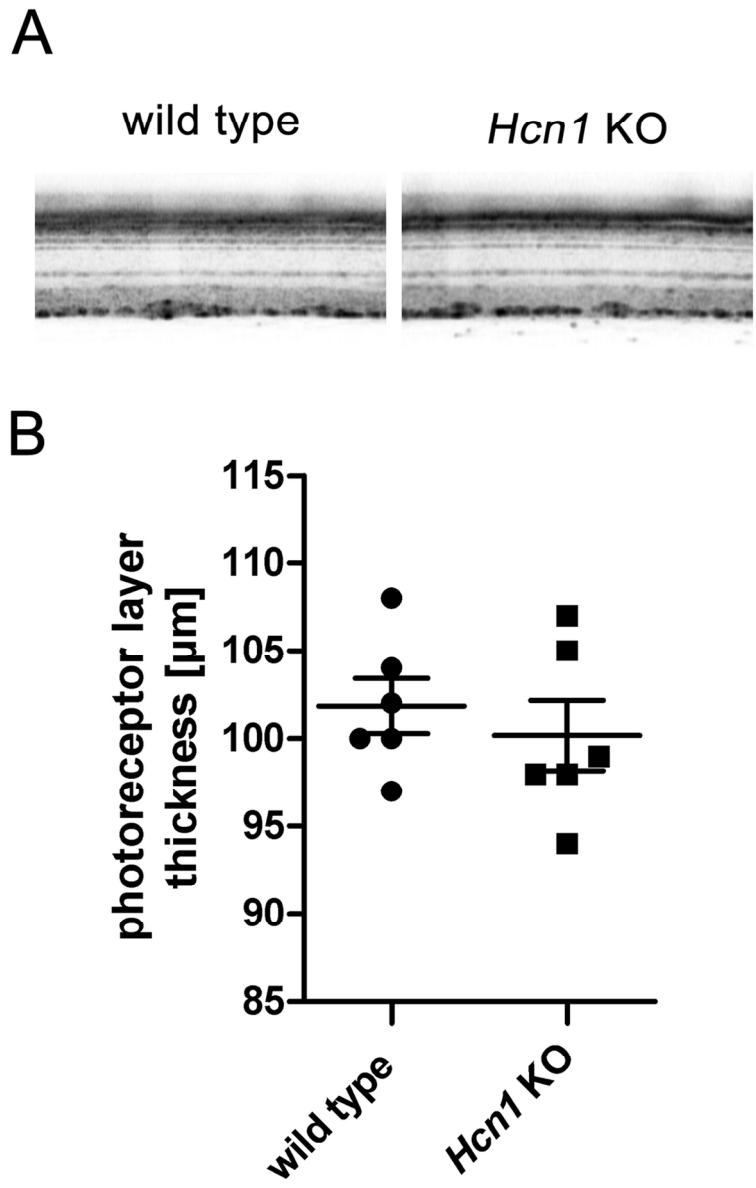

Figure S1. Knockout of Hcn1 has no major effect on retinal morphology and photoreceptor layer thickness.
97x153mm (300 x 300 DPI)

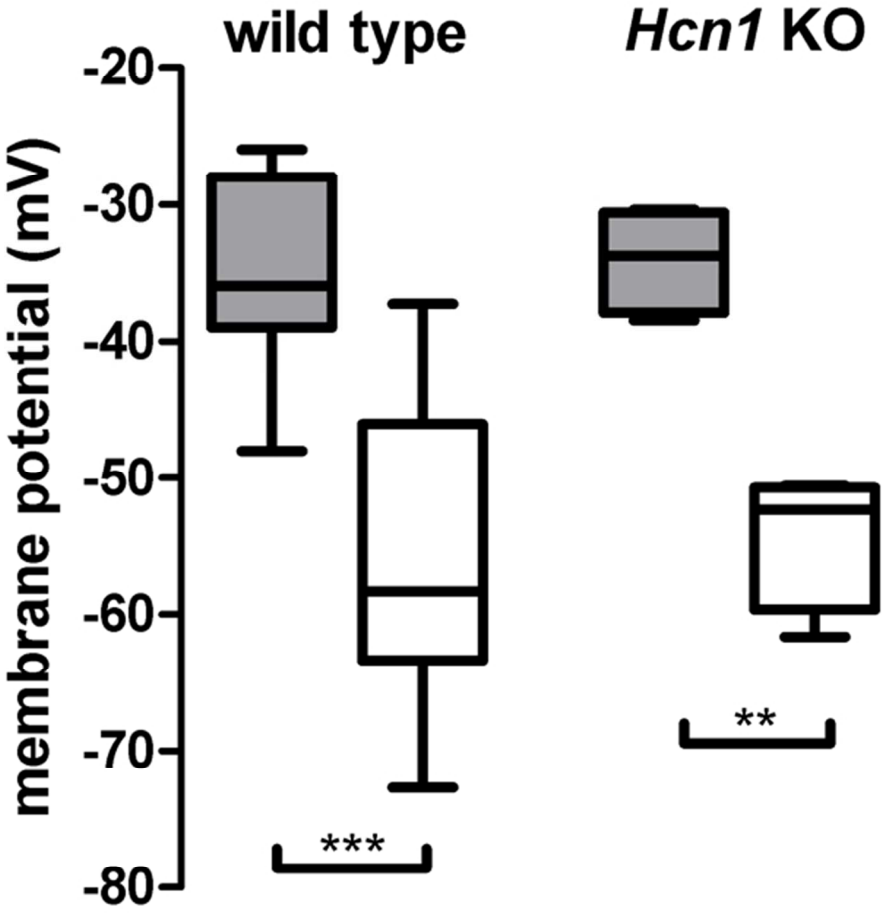

Figure S2. Knockout of Hcn1 has no major effect on the membrane potential of rod photoreceptors.
57x57mm (300 x 300 DPI)

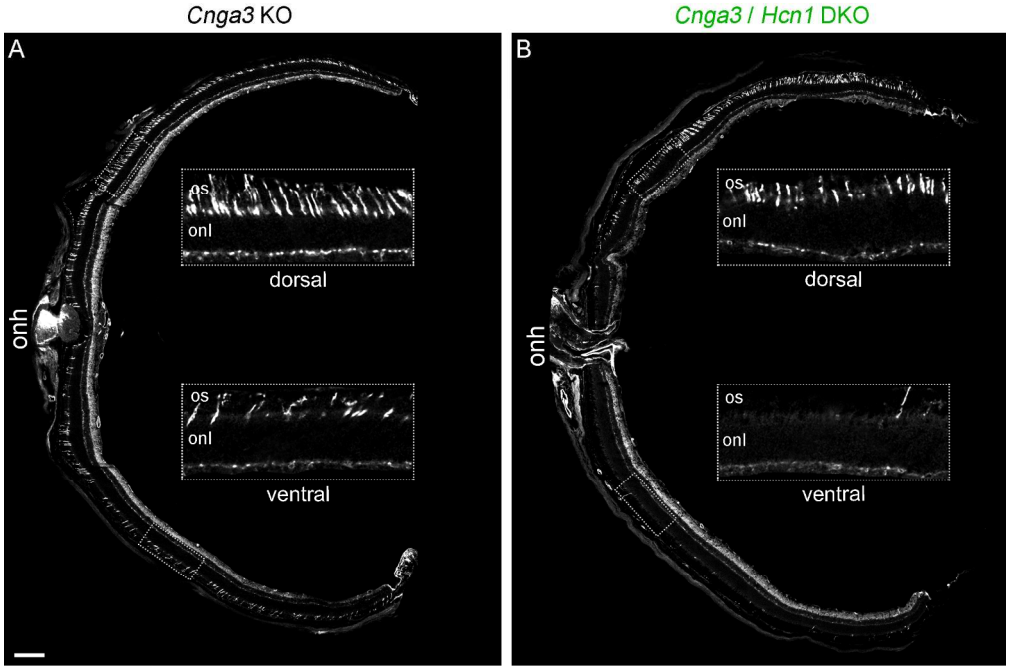

Figure S3. Knockout of Hcn1 enhances photoreceptor degeneration in Cnga3-deficient mice.
199x133mm (300 x 300 DPI)

Review